Concentration dependence of structural and bonding properties of liquid Tl-Se alloys by *ab initio* molecular dynamics simulations

Akihide Koura and Fuyuki Shimojo
Department of Physics, Kumamoto University, Kumamoto 860-8555, Japan
(Received 13 June 2008; published 9 September 2008)

The structural and electronic properties of liquid Tl_xSe_{1-x} for $0 \leq x \leq 1$ are investigated by means of *ab initio* molecular dynamics simulations. It is shown that calculated structure factors are in good agreement with experiments over the whole range of composition. It is confirmed from calculated electronic densities of states that the liquid Tl-Se alloys have semiconducting properties for Tl concentrations not exceeding the stoichiometric composition ($x=2/3$), while they are metallic for $x>2/3$. In Se-rich composition range, Se atoms form chain molecules, whose average length becomes shorter with increasing Tl concentration. In the equiatomic liquid Tl-Se alloy, short Se chains, mostly negatively charged Se_2 dimers, coexist with a few Se ions, while most of Se atoms exist as ions at the stoichiometric composition. Based on a population analysis, we discuss the concentration dependence of the bonding properties in comparison with that in liquid alkali-metal chalcogenides.

DOI: 10.1103/PhysRevB.78.104203 PACS number(s): 61.20.Ja, 71.22.+i, 71.15.Pd

I. INTRODUCTION

Liquid Se exhibits semiconducting behavior similar to that of the crystalline phase in a wide range of pressure and temperature. It consists of chain molecules with covalent bonds between Se atoms.[1] The effects of the addition of Tl metal on the electronic properties have been studied experimentally so far.[2–4] When the Tl concentration x is relatively low ($x \leq 0.5$), the electrical conductivity increases with increasing x while keeping the semiconducting properties. At the stoichiometric composition of Tl_2Se ($x=0.67$), a deep minimum occurs in the concentration dependence of the electrical conductivity. For higher Tl concentrations with $x>0.67$, the liquid Tl-Se alloys show metallic properties.

These changes in the electronic properties due to the addition of Tl atoms must be closely related to the composition dependence of the structure. Usuki *et al.*[5] have carried out neutron-diffraction experiments to investigate the structure of the liquid Tl-Se system over the whole concentration range. They found that the covalent-type Se polymeric structure is preserved in Se-rich composition range, while the short-range structure is similar to that of pure liquid Tl when the Tl concentration is higher than the stoichiometric composition. Lague *et al.*[6] have also obtained the neutron total structure factors for liquid Tl_xSe_{1-x} for $x=0.4$, 0.5, and 0.67. They suggested that the formation of Se_n^{2-} polyanions is responsible for the low conductivity and high thermopower. Using the technique of neutron scattering and isotopic substitution, Barnes and Guo[7] have obtained the partial structure factors of the stoichiometric liquid Tl_2Se alloy. Since the observed interatomic distances are consistent with the ionic radii of Tl^+ and Se^{2-}, and the partial structure factors are very similar to those obtained theoretically using screened ionic potentials, they concluded that the properties of liquid Tl_2Se are well understood in terms of the basic ionic picture. The partial structure factors of the equiatomic liquid TlSe alloy have been measured by Barnes *et al.*[8] using the similar technique to that of Barnes and Guo. Their experimental results confirmed the formation of Se polyanions in the liquid state.

The temperature dependence of the specific heat of the liquid Tl-Se system has been measured over a wide composition range by Kakinuma *et al.*[9] They discussed the variation of the thermodynamic properties in relation to the structural changes. A thorough experimental investigation into the molar volume and compressibility has been carried out by Tsuchiya.[10] He found that there exists a cusplike local maximum at Tl_2Se in the concentration dependence of the molar volume and compressibility. Recently, Ohmasa *et al.*[11] have found that the Tl-Se mixtures exhibit unusual wetting behavior on a silica substrate, which would be due to a peculiarity of the interatomic interaction in the Tl-Se system. They studied wetting dynamics in the liquid Tl-Se mixtures contacting a silica wall.[12] They also investigated the wetting phenomena not only in the thermal equilibrium state but also in nonequilibrium states.[13]

As stated above, the structural, electronic, and thermodynamic properties of the liquid Tl-Se system have been extensively studied by experimental methods. For further understanding the properties of these liquid alloys, theoretical methods based on the *ab initio* technique would be powerful. However, only a few *ab initio* studies on this kind of alloys have been reported so far. An *ab initio* pseudopotential calculation using density-functional theory has been carried out to investigate the electronic properties of crystalline TlSe.[14] Although we are unaware of *ab initio* studies on the liquid Tl-Se system, the properties of disordered phases of In-Se mixtures have been investigated from first principles. *Ab initio* molecular dynamics (MD) simulations have been used to study the structural and electronic properties of liquid In_xSe_{1-x} for two concentrations of $x=0.5$ and 0.8.[15] The structure of amorphous In_xSe_{1-x} with $x=0.4$, 0.5, and 0.6 has been studied by a first-principles tight-binding MD technique.[16]

In this study, we investigate the structure and electronic states of the liquid Tl-Se alloys by *ab initio* MD simulations. We give a detailed comparison of calculated results with the experimental data, and clarify the concentration dependence of the structural and bonding properties of the liquid Tl-Se alloys. Especially, the change of the chain structure of Se

TABLE I. Tl concentrations x, temperatures T, and number densities ρ used in MD simulations for liquid Tl_xSe_{1-x}.

x	T (K)	ρ(Å^{-3})
0.00	600	0.0295
0.15	760	0.0304
0.25	600	0.0313
0.40	670	0.0313
0.50	680	0.0313
0.67	770	0.0292
0.85	830	0.0270
1.00	770	0.0325

atoms due to the addition of Tl metal is studied in detail. In *ab initio* investigations of liquid alkali-metal selenides and alkali-metal tellurides,[17–19] the bonding properties between chalcogen atoms (Se-Se or Te-Te) have been discussed thoroughly as a function of the alkali-metal concentration. It is therefore interesting to compare the composition dependence of the chalcogen-chain structure in the liquid Tl-Se system with that in the liquid alkali-metal chalcogenides.

II. METHOD OF CALCULATION

The electronic states were calculated using the projector-augmented-wave (PAW) method[20,21] within the framework of the density-functional theory (DFT) in which the generalized gradient approximation (GGA) (Ref. 22) was used for the exchange-correlation energy. The plane-wave cutoff energies are 18 and 85 Ry for the electronic pseudowave functions and the pseudocharge density, respectively. The energy functional was minimized using an iterative scheme.[23,24] The Γ point was used for Brillouin-zone sampling. Projector functions of the s, p, and d types were generated for the 4s, 4p, and 4d states of Se, and the 5d, 6s, and 6p states of Tl. The cutoff radii r_{cl}, beyond which the pseudowave functions coincide with the all-electron wave functions, were chosen as r_{cl}=2.4 and 2.8 a.u. for Se and Tl, respectively. In the construction of the PAW data sets, two reference energies were used except for the 4d states of Se. By investigating the energy dependence of the logarithmic derivatives of the pseudowave functions, we verified that our data sets have good transferability, and do not possess any ghost states in the energy range considered.

Molecular dynamics simulations were carried out at the same compositions and temperatures as those used in the neutron-diffraction measurements by Usuki *et al.*[5] to compare calculated results with their experimental results. Atomic densities used in our simulations were taken from the experiments.[10] The Tl concentrations, temperatures, and atomic number densities are listed in Table I. Note that there are the liquid-liquid two-phase regions in the binary phase diagram for the Tl-Se system.[25] Actually, the state at x=0.85 and T=830 K exists within such region, which means that one of the neutron-diffraction measurements was carried out for a phase separated liquid. Nevertheless, Usuki *et al.* have reported that no splitting pattern appears on the structure factor at x=0.85 and T=830 K. To see if our simulation method reproduces the behavior of the phase separation, we dare simulate the phase separated state at x=0.85. For each composition, we used a 128-atom system in a cubic supercell with periodic boundary conditions. Using the Nosé-Hoover thermostat technique,[26,27] the equations of motion were solved via an explicit reversible integrator[28] with a time step of Δt=2.4 fs. The quantities of interest were obtained by averaging over 9.6 ps after an initial equilibration taking at least 1.2 ps.

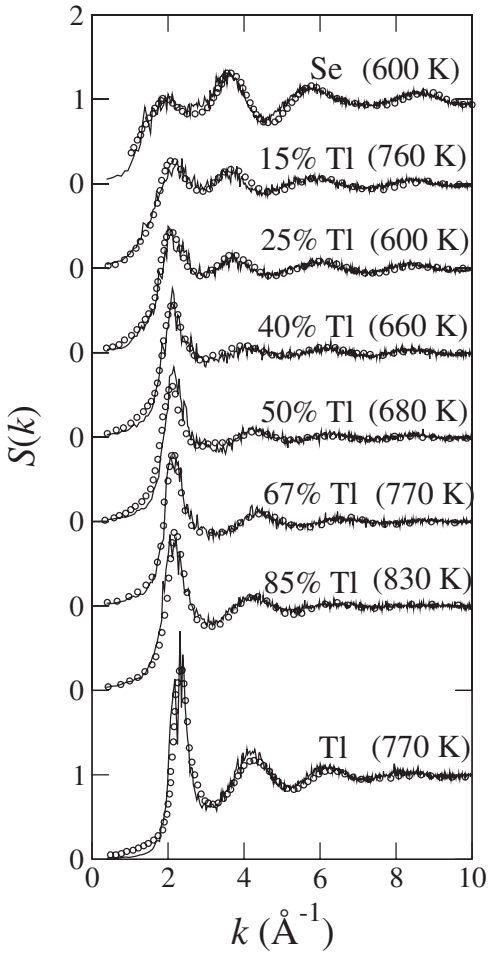

FIG. 1. Total structure factors $S(k)$ of liquid Tl-Se alloys; the solid lines and open circles show the calculated and experimental (Ref. 5) results, respectively.

III. RESULTS AND DISCUSSION

A. Structure factors

The comparison of calculated total structure factors $S(k)$ with the experimental data[5] is shown in Fig. 1. We calculated $S(k)$ from the partial structure factors $S_{\alpha\beta}(k)$, shown in Fig. 2, with the neutron-scattering lengths. It is seen that the theoretical results are in good agreement with the experiments for the whole range of composition. With increasing Tl concentration, the first peak shifts toward larger k from about 2.0 Å^{-1} in pure liquid Se to about 2.3 Å^{-1} in pure liquid Tl, while increasing the peak height. When the Tl concentration

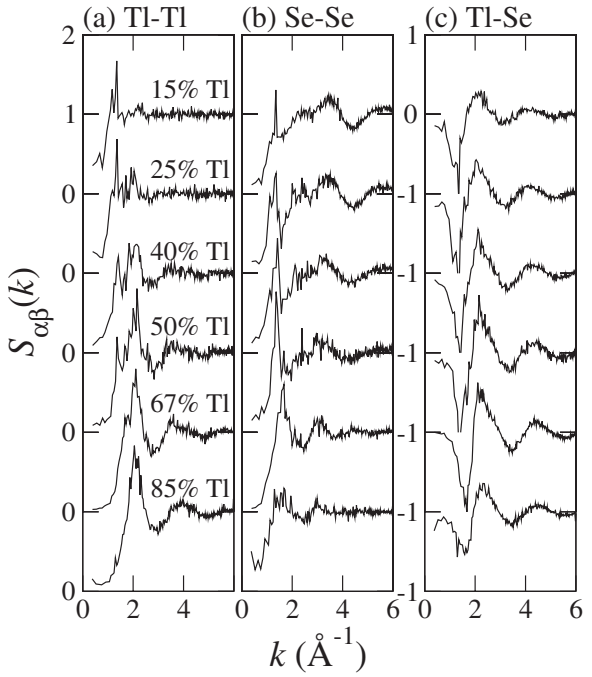

FIG. 2. Calculated partial structure factors $S_{\alpha\beta}(k)$ of liquid Tl-Se alloys for α-β=(a) Tl-Tl, (b) Se-Se, and (c) Tl-Se.

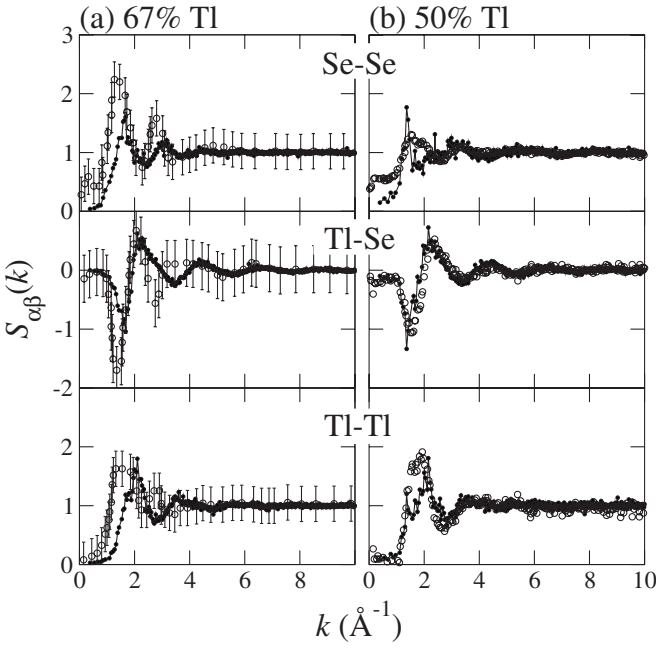

FIG. 3. Partial structure factors $S_{\alpha\beta}(k)$ of liquid (a) Tl_2Se and (b) TlSe alloys. The calculated results (solid circles) are compared with the experimental results obtained by diffraction techniques with isotopic substitution (Refs. 7 and 8) (open circles).

is increased from x=0.0 to 0.67, the second peak moves toward larger k, and it moves toward smaller k for further increase of x. The positions of the second peak for x=0.0, 0.67, and 1.0 are about 3.6, 4.4, and 4.2 Å^{-1}, respectively. The height of the second peak decreases markedly with increasing Tl concentration for $x<0.5$, while it increases for $x>0.5$. The third peak shows similar concentration dependence to that of the second peak. These features are common to both the calculated and experimental $S(k)$.

The Ashcroft-Langreth partial structure factors $S_{\alpha\beta}(k)$ are shown in Fig. 2. For $x\leq 0.5$, both $S_{\mathrm{TlTl}}(k)$ and $S_{\mathrm{SeSe}}(k)$ have peaks at about 1.3 Å^{-1}. Since the negative dip exists at the same wave vector in $S_{\mathrm{TlSe}}(k)$, there exists no peak around 1.3 Å^{-1} in the total $S(k)$ due to the cancellation. These peaks and dip in $S_{\alpha\beta}(k)$ arise from charge ordering on an intermediate length scale of a few angstroms.

In the liquid alkali-metal chalcogenides, there also exists charge ordering on a similar length scale.[17–19] However, the peaks in the chalcogen-chalcogen correlations are clearer and sharper than those in the Tl-Se alloys especially at the equiatomic composition. This structural difference would come from the amount of charge transfer to chalcogen atoms. As will be discussed later, the charge transfer from Tl to Se occurs incompletely in the Tl-Se alloys, while the electrons of alkali-metal atoms are transferred almost completely to chalcogen atoms.

In $S_{\mathrm{TlTl}}(k)$, a peak grows at about 2.0 Å^{-1} with increasing x. At x=0.4, another peak appears around 3.5 Å^{-1}, and shifts toward larger k when x is increased. In $S_{\mathrm{SeSe}}(k)$, the position of the peak at about 1.3 Å^{-1} moves to about 1.7 Å^{-1} when x changes from 0.5 to 0.67. For $x\leq 0.5$, there are peaks at about 2.4 and 3.5 Å^{-1}, and they are merged into one peak at about 3.1 Å^{-1} for $x\geq 0.67$. In $S_{\mathrm{TlSe}}(k)$, the position of the negative dip around 1.3 Å^{-1} moves to about 1.7 Å^{-1} between x=0.5 and 0.67 corresponding to the peak shift in $S_{\mathrm{SeSe}}(k)$. Both peaks at about 2.1 and 4.0 Å^{-1} shift toward larger k with increasing x. The heights of these peaks are highest at x=0.67.

Here, we should mention the structure at x=0.85 in connection with the phase separation. Although the liquid alloy at x=0.85 and T=830 K must separate into two phases as described in Sec. II, we see no evidence of the phase separation in the both experimental and calculated total $S(k)$ shown in Fig. 1. It is, however, noted that there are some indications of the phase separation in the partial structure factors. As clearly seen in Fig. 2(b), $S_{\mathrm{SeSe}}(k)$ at x=0.85 has higher values for $k<1$ Å^{-1} compared with those for $x\leq 0.67$, and increases with decreasing k. Also, $S_{\mathrm{TlTl}}(k)$ at x=0.85 seems to exhibit similar behavior for $k<1$ Å^{-1} as $S_{\mathrm{SeSe}}(k)$ [Fig. 2(a)]. These results indicate that there exist long-range fluctuations in the density distribution of Se and Tl arising from structural instability in the liquid. Due to the system size, we may not be able to reproduce the phase separation completely in our simulations. Still, we can see that the calculated structure of the liquid alloy at x=0.85 and T=830 K shows some indications of the phase separation, even though the total $S(k)$ has no evidence.

The partial structure factors of the liquid Tl_2Se and TlSe alloys have been obtained by diffraction techniques with isotopic substitution.[7,8] It is, therefore, worthwhile comparing these experimental $S_{\alpha\beta}(k)$ with our theoretical results as shown in Fig. 3. The calculated and experimental $S_{\alpha\beta}(k)$ are shown by the solid and open circles, respectively. Since there is great difficulty in determining the partial quantities from experiments, it may not be expected that the experimental results are superior to the theoretical ones. On the other hand, we do not assert that the theoretical results are thoroughly

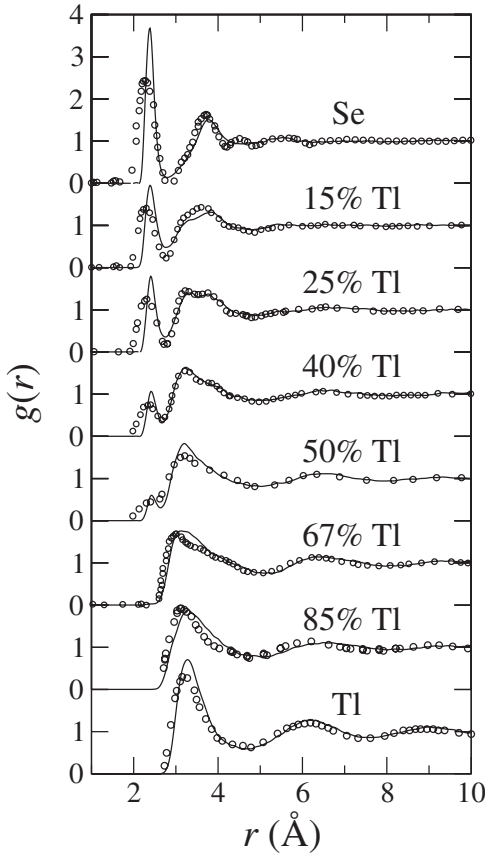

FIG. 4. Total pair distribution functions $g(r)$ of liquid Tl-Se alloys. The solid lines and open circles show the calculated and experimental (Ref. 5) results, respectively.

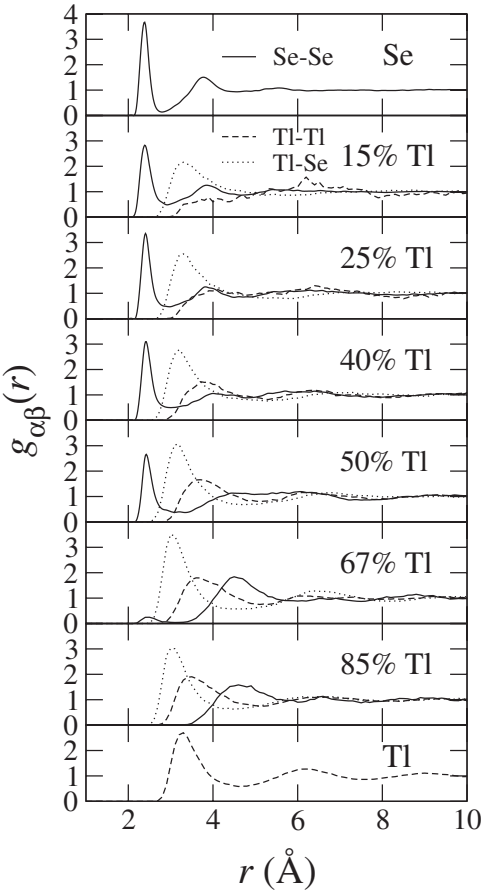

FIG. 5. Calculated partial pair distribution functions $g_{\alpha\beta}(k)$ of liquid Tl-Se alloys. The solid, dashed, and dotted lines show the correlations for α-β=Se-Se, Tl-Tl, and Tl-Se, respectively.

accurate because the approximations in the calculation method, such as GGA, could possibly be inadequate. Considering these facts, the difference between both results is reasonable. It seems that the agreement for the liquid TlSe alloy [Fig. 3(b)] is better than that for the Tl_2Se alloy [Fig. 3(a)], which would come from the difference in the experimental techniques.

B. Pair distribution functions

In Fig. 4, the calculated total pair distribution functions $g(r)$ are compared with the experimental results.[5] We see that the agreement between them is reasonably good for all compositions. The first peak at about 2.3 Å becomes lower with increasing Tl concentration, and disappears at $x=0.67$, while its position is unchanged for $x \leq 0.5$. Although the second peak exists clearly at about 3.8 Å in pure liquid Se, its height decreases by the addition of Tl atoms. Instead, a peak grows around 3.3 Å with increasing x.

Figure 5 shows the partial pair distribution functions $g_{\alpha\beta}(r)$. In pure liquid Se, $g_{\mathrm{SeSe}}(r)$ reflects the chain structure. The first peak corresponds to the correlation between nearest neighbors within a chain, while the second peak is mainly contributed by next-nearest neighbors within a chain. Atomic correlations between distinct chains have also some contribution to $g_{\mathrm{SeSe}}(r)$ beyond 3 Å. The clear minimum at about 2.8 Å indicates that Se chains do not frequently interact with each other. By the addition of Tl atoms, the minimum becomes shallower, and the second peak shifts slightly toward larger r in $g_{\mathrm{SeSe}}(r)$, while the position of the first peak remains the same. These changes suggest an increase of interchain interaction due to the presence of Tl atoms. The profiles of $g_{\mathrm{SeSe}}(r)$ for $x \geq 0.67$ are completely different from those for $x \leq 0.5$, which would indicate that the chain structure vanishes when the Tl concentration is not less than the stoichiometric composition. It is clearly seen that the first peak at about 2.3 Å in the total $g(r)$ comes from the Se-Se correlation in the chain structure as pointed out by the previous studies.[5,6,8]

At $x=0.15$, $g_{\mathrm{TlSe}}(r)$ has a first peak at about 3.3 Å followed by a broad profile. Its position shifts slightly toward smaller r with increasing x, while becoming higher. This Tl-Se correlation gives the peak around 3.3 Å in the total $g(r)$. While there are no clear peaks in $g_{\mathrm{TlTl}}(r)$ for $x \leq 0.25$, there appears a broad first peak at about 3.8 Å when the Tl concentration is increased to $x=0.4$. For further increase of Tl concentration, the first peak moves toward smaller r, and becomes gradually higher. In pure liquid Tl, the position of the first peak is about 3.3 Å.

The concentration dependence of $g_{\mathrm{SeSe}}(r)$ in the liquid alkali-metal selenides[17] is similar to that in the current system when the alkali-metal concentration is lower ($x \leq 0.2$). However, at the equiatomic concentration, $g_{\mathrm{SeSe}}(r)$'s in the

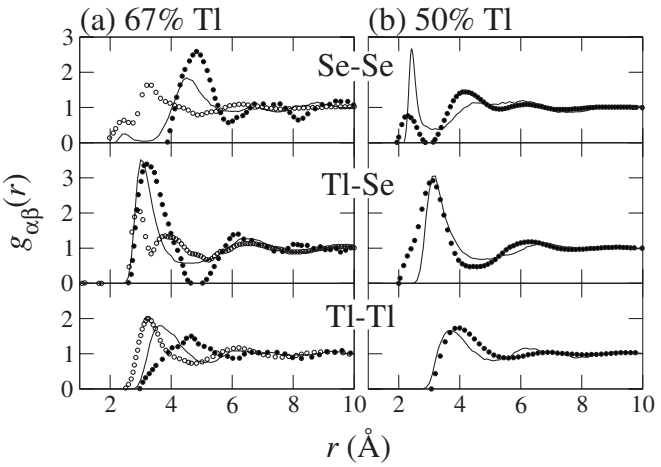

FIG. 6. Partial pair distribution functions $g_{\alpha\beta}(k)$ of liquid (a) Tl_2Se and (b) TlSe alloys. The calculated results (solid lines) are compared with the experimental results obtained by diffraction techniques with isotopic substitution (Ref. 7 and 8) (solid circles), and those obtained by neutron-diffraction measurements (Ref. 5) (open circles).

two liquid systems are rather different from each other. In the profile of $g_{SeSe}(r)$ for liquid $Rb_{0.5}Se_{0.5}$, there exists a wide deep valley between the sharp first peak and the wide-ranging second peak at about 6 Å, which reflects the existence of stable Se_2^{2-} dimers. On the other hand, the minimum of $g_{SeSe}(r)$ around 3.2 Å for liquid $Tl_{0.5}Se_{0.5}$ is fairly shallow as shown in Fig. 5 This would mean that the structure of dimers or short chains is unstable, and Se covalent bonds exchange frequently in the liquid Tl-Se system even at the equiatomic composition.

The comparison with the experimental results for the liquid Tl_2Se and TlSe alloys is shown in Fig. 6. The solid lines show the calculated $g_{\alpha\beta}(r)$. The solid and open circles show the experimental results obtained by diffraction techniques with isotopic substitution[7,8] and by neutron-diffraction measurements,[5] respectively. It is seen that the difference between the two experimental results is significant as shown in Fig. 6(a), which would be caused by the fact that $g_{\alpha\beta}(r)$'s displayed with the open circles were obtained based on the assumption that each partial structure is independent of the relative abundance of the constituent elements in the alloys.[5] Although there are some discrepancies, the overall agreement between the solid lines and the solid circles is satisfactory in the sense discussed in Sec. III A, which implies that our *ab initio* calculations support the experimental results with isotopic substitution techniques.

C. Electronic densities of states

Figure 7 shows the electronic densities of states (DOS) $D(E)$ of liquid Tl_xSe_{1-x}. The origin of energy is taken to be the Fermi level. At $x=0.0$, $D(E)$ has a deep dip at the Fermi level corresponding to the semiconducting properties of liquid Se. Although $D(E)$'s for $0.15 \leq x \leq 0.5$ have finite values at the Fermi level, which conforms to the increase of the electrical conductivity by the addition of Tl atoms, the existence of the clear dip at the Fermi level means that these

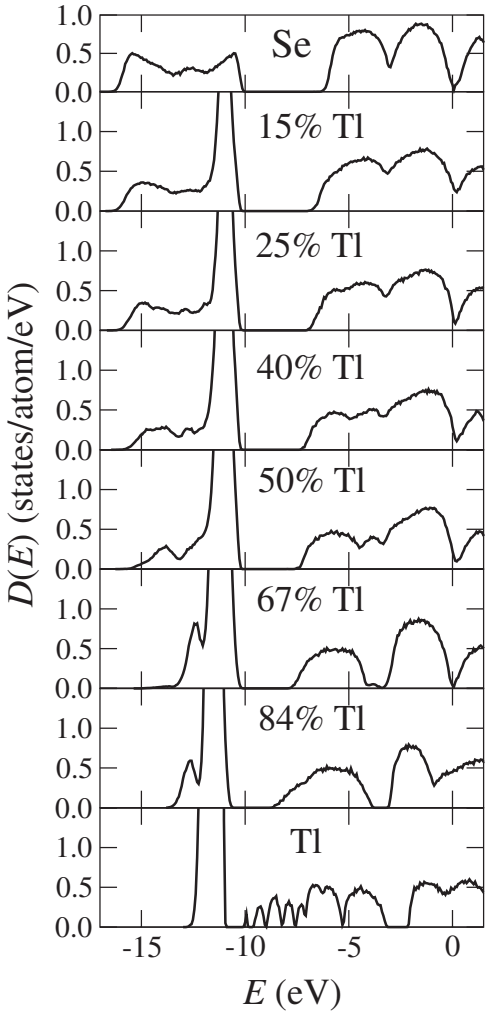

FIG. 7. Total electronic densities of states $D(E)$ of liquid Tl-Se alloys. The origin of energy is taken to be the Fermi level ($E_F=0$).

liquid alloys keep semiconducting properties. At the stoichiometric composition of $x=0.67$, the dip becomes deeper again, which is consistent with the fact that a minimum occurs in the concentration dependence of the electrical conductivity. We see that the system has metallic properties for $x \geq 0.84$, as there is no dip at the Fermi level. These changes in $D(E)$ due to the addition of Tl atoms are in qualitative agreement with the experimental observations.[2–4]

Figure 8 shows the concentration dependence of the partial DOS $D_\alpha^l(E)$ with the angular momentum l around α-type atoms.[29] It is seen from Figs. 7 and 8 that the electronic states below −10 eV consist of the 4*s* states of Se and the 5*d* states of Tl, whereas those above −8 eV are mainly formed by the 4*p* states of Se and the 6*s* states of Tl. The 6*p* states of Tl also give some contributions to the electronic states above −5 eV. For lower Tl concentrations ($x<0.5$), there are two broad peaks at about −4 and −1 eV in $D_{Se}^{4p}(E)$ corresponding to bonding and nonbonding states, respectively, in the chain structure. We see that $D_{Se}^{l}(E)$ for $x \leq 0.5$ is largely different from that for $x \geq 0.67$. This is consistent with the structural changes we have seen in Fig. 5. It is found that the profile of $D_{Tl}^{5d}(E)$ spreads over only a narrow energy range and has weak composition dependence. Also, it is seen that the me-

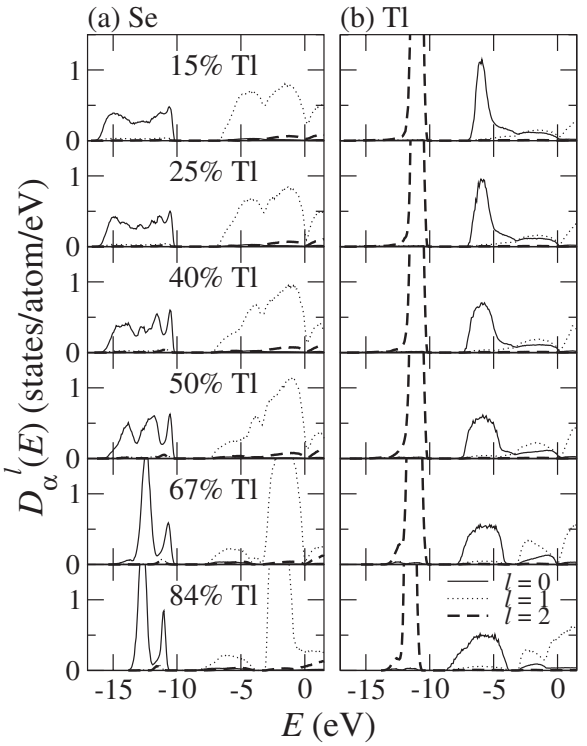

FIG. 8. Partial electronic densities of states $D_\alpha^l(E)$ of liquid Tl-Se alloys for α=(a) Se and (b) Tl. The solid, dotted, and dashed lines show $D_\alpha^l(E)$ for l=0, 1, and 2, respectively.

tallic properties for $x \geq 0.84$ originate mainly from the 6p states of Tl.

In the liquid alkali-metal chalcogenides, the partial DOS for alkali-metal atoms has very small values over the energy range where the p states of chalcogen atoms exist, when the alkali-metal concentrations are not exceeding 0.5.[17–19] This fact suggests that nearly complete charge transfer from alkali-metal to chalcogen atoms occurs. On the other hand, since $D_{\mathrm{Tl}}^{6s}(E)$ has fairly large values even for lower Tl concentrations as seen in Fig. 8(b), we see that the charge transfer from Tl to Se atoms is incomplete in the liquid Tl-Se alloys. Moreover, in the alkali-metal chalcogenides at the equiatomic concentration, the partial DOS for the p states of chalcogen atoms has three sharp peaks below the Fermi level,[17–19] which reflects the electronic states in Se_2^{2-} dimers. However, $D_{\mathrm{Se}}^{4p}(E)$ for the liquid Tl-Se system at x=0.5 consists of only one large peak around −1 eV with a broad tail toward lower energies as shown in Fig. 8(a). Although a small peak is recognized at about 4 eV, this partial DOS is dissimilar to the electronic states in the stable dimers.

D. Chain structure of Se atoms

To investigate the change in the chain structure, we obtained the ratio $d(n)$ of the number of Se atoms coordinated with n Se atoms to the total number of Se atoms by counting the number of atoms inside the sphere of a radius R centered at each atom. We used the first minimum position, 2.8 Å, of $g_{\mathrm{SeSe}}(r)$ as R. The Tl-concentration dependence of $d(n)$ is shown in Fig. 9. It is seen that almost all Se atoms have

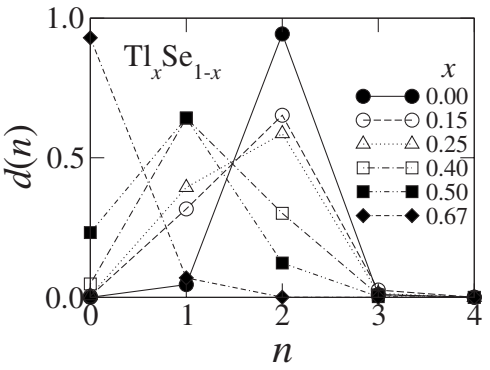

FIG. 9. Tl-concentration x dependence of Se-Se coordination-number distribution $d(n)$ in liquid Tl-Se alloys.

twofold coordination in pure liquid Se. With increasing Tl concentration up to x=0.4, the ratio of twofold-coordinated Se atoms decreases, and that of onefold-coordinated Se atoms increases. This concentration dependence clearly shows that Se chains are shortened by the addition of Tl atoms. When the Tl concentration is increased from 0.4 to 0.5, the number of onefold-coordinated Se atoms is unchanged, while the ratio of twofold-coordinated Se atoms keeps decreasing. Note that $d(0)$ has a finite value, which indicates that there exist negatively charged Se ions neighboring to only Tl atoms at the equiatomic concentration. At the stoichiometric composition (x=0.67), $d(2)$ and $d(1)$ become nearly zero, and $d(0)$ has a high value, i.e., most of Se atoms exist as ions.

In Table II, we show the concentration dependence of the average length of Se chains calculated by connecting up Se atoms with atomic distances less than R. The ratio of Se ions estimated from $d(0)$ at each concentration is also listed. It is quite natural that the average length of Se chains decreases with increasing Tl concentration. It is, however, seen that the average length, 2.5, at the equiatomic composition is greater than the ideal value, 2.0. This means that there exist short Se chains as well as Se_2 dimers and Se ions in liquid $Tl_{0.5}Se_{0.5}$.

In the liquid alkali-metal selenides,[17] the average length of Se chains also decreases with increasing alkali-metal concentration. However, the average length at the equiatomic composition is nearly the ideal value, and almost all Se atoms form Se_2^{2-} dimers, because the charge transfer occurs almost completely.

E. Bond-overlap populations

We used population analysis[30,31] to clarify the change in the bonding properties due to the addition of Tl atoms. By

TABLE II. Tl-concentration x dependence of the average length of Se chains, l_{chain}, and the ratio of Se ions, w(ion).

x	l_{chain}	w(ion)
0.15	6.7	0.00
0.25	5.0	0.00
0.40	3.1	0.04
0.50	2.5	0.22
0.67	1.0	0.93
0.85	1.0	1.00

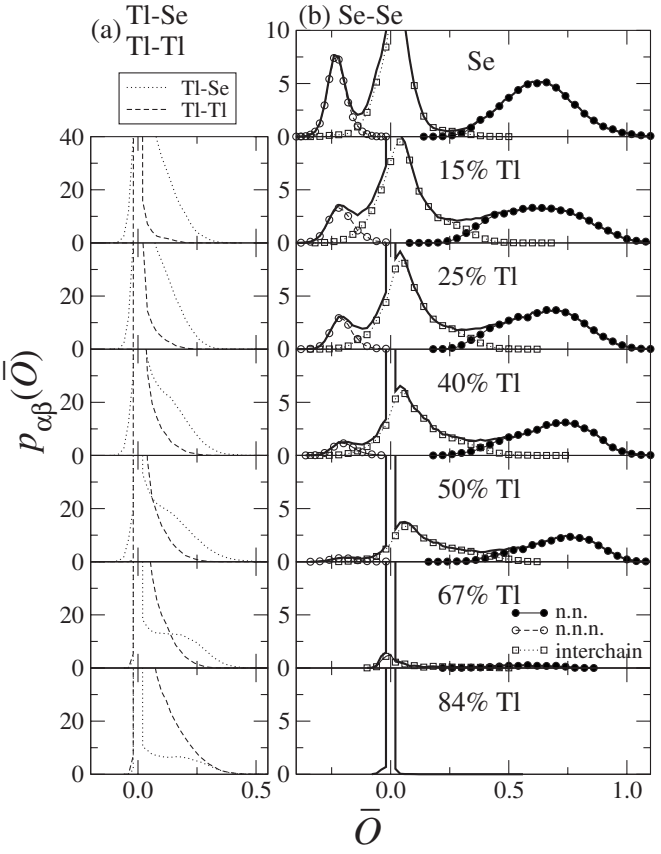

FIG. 10. Distributions $p_{\alpha\beta}(\bar{O})$ of overlap populations $O_{i\in\alpha,j\in\beta}$ for α-β=(a) Tl-Se and Tl-Tl, and (b) Se-Se. The solid and open circles show the contributions to $p_{\mathrm{SeSe}}(\bar{O})$ from nearest-neighbor (n.n.) atoms and next-nearest-neighbor (n.n.n.) atoms, respectively, within a chain, while the open squares show the interchain contribution to $p_{\mathrm{SeSe}}(\bar{O})$.

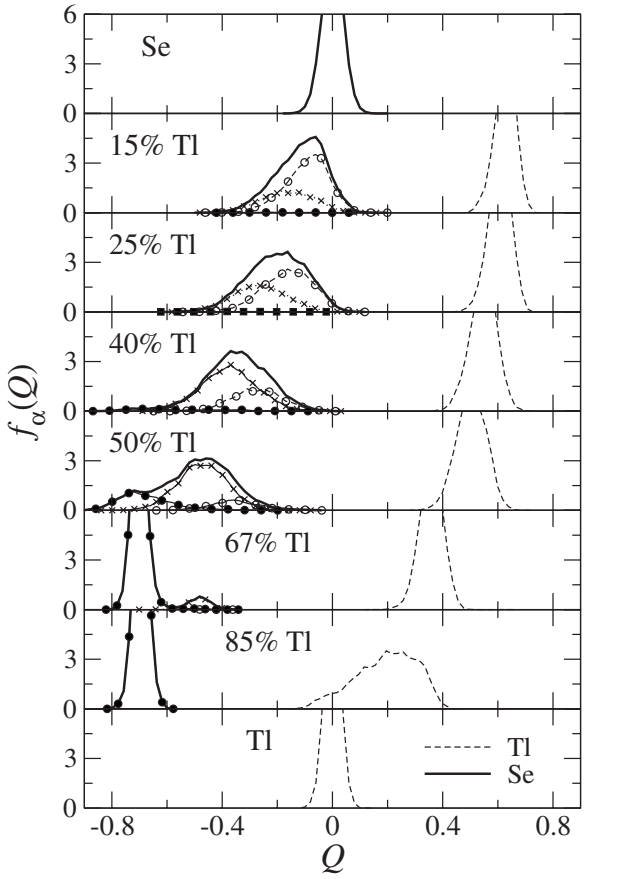

FIG. 11. Distributions $f_\alpha(Q)$ of gross charges $Q_{i\in\alpha}$. The solid and dashed lines show $f_{\mathrm{Se}}(Q)$ and $f_{\mathrm{Tl}}(Q)$, respectively. The open circles and crosses show the contributions to $f_{\mathrm{Se}}(Q)$ from Se atoms coordinated to two and one neighboring Se, respectively, while the solid circles show the contributions to $f_{\mathrm{Se}}(Q)$ from Se atoms that have no neighboring Se.

expanding the electronic wave functions in an atomic-orbital basis set,[29,32,33] we obtained the overlap population O_{ij} between the ith and jth atoms and the gross charge Q_i for the ith atom.[30] See details of the calculation in Refs. 17 and 29. Here we mention that the charge spillage,[32] which estimates the error in the expansion, is only 0.1%, indicating that our basis orbitals are of high quality.

Figure 10 shows the time-averaged distributions $p_{\alpha\beta}(\bar{O})$ (Ref. 34) of the overlap populations $O_{i\in\alpha,j\in\beta}$ which give a semiquantitative estimate of the strength of bonding between atoms. We see from Fig. 10(a) that the distribution ranges of $p_{\mathrm{TlSe}}(\bar{O})$ and $p_{\mathrm{TlTl}}(\bar{O})$ spread over larger $\bar{O}$ with increasing Tl concentration. The fact that pairs of Tl and Se atoms have finite values of the overlap population indicates that the interaction between Tl and Se atoms is not purely ionic. The values of $p_{\mathrm{TlSe}}(\bar{O})$ for $\bar{O}>0.0$ become smaller for larger Tl concentrations, because the average number of Se atoms around each Tl atom is smaller.

In the distribution of $p_{\mathrm{SeSe}}(\bar{O})$ in pure liquid Se, there are two peaks at about $\bar{O}=0.6$ and -0.2 except around $\bar{O}=0.0$ as shown in Fig. 10(b). By identifying Se chains in the liquid alloys, we examine $p_{\mathrm{SeSe}}(\bar{O})$ in connection with the chain structure of Se atoms. The solid circles show the time-averaged distribution of the overlap populations for pairs of nearest-neighbor Se atoms within a chain, which has the peak at the larger $\bar{O}\sim 0.6$ because of the σ-type covalent bonding between atoms. Since the antibonding interaction exists between the lone-pair states of next-nearest-neighbor Se atoms within a chain, those pairs of Se atoms give the peak at the negative $\bar{O}\sim -0.2$ as displayed by the open circles. The contribution from pairs of Se atoms belonging to different chains, shown by the open squares, has a peak at $\bar{O}\sim 0.1$. A characteristic feature in pure liquid Se is that these three distributions are well separated to each other by clear minima at about $\bar{O}=0.2$ and -0.1, reflecting the clear chain structure. With increasing Tl concentration, the two minima become shallower because Se chains interact more frequently with each other due to the excess electronic charges transferred from Tl atoms. Even at the equiatomic concentration, the distribution of $p_{\mathrm{SeSe}}(\bar{O})$ is qualitatively the same as those for lower Tl concentrations, though the peak at the negative $\bar{O}\sim -0.2$ almost disappears. For $x\geq 0.64$, $p_{\mathrm{SeSe}}(\bar{O})$ does not have finite values at finite $\bar{O}$, which means that the chain structure vanishes.

In the liquid alkali-metal selenides,[17] $p_{\mathrm{SeSe}}(\bar{O})$ at the equiatomic concentration has a qualitatively different profile from those at lower alkali-metal concentrations, due to the formation of dimers. The distribution from nearest neighbors shifts toward larger $\bar{O}$, and has a peak at about $\bar{O}=1.0$, which shows a stronger chemical bonding in dimers. Also, the contribution from the interchain interaction almost disappears, i.e., the dimer-dimer interaction occurs infrequently.

F. Mulliken charges

Figure 11 shows the time-averaged distributions $f_{\alpha}(Q)$ (Ref. 35) of $Q_{i\in\alpha}$ for α-type atoms. It is quite natural that, in pure liquids ($x=0.0$ and 1.0), $f_{\alpha}(Q)$ has a symmetric distribution around $Q=0.0$. At $x=0.15$, $f_{\mathrm{Tl}}(Q)$ has a peak at about $Q=0.6$, which is much smaller than the ideal value, 1.0. The peak position shifts toward smaller Q with increasing Tl concentration, i.e., the number of electrons around each Tl atom increases as the Tl concentration increases. While the profile of $f_{\mathrm{Tl}}(Q)$ is symmetric for $x\leq 0.67$, $f_{\mathrm{Se}}(Q)$ has an asymmetric distribution. We decompose $f_{\mathrm{Se}}(Q)$ into three contributions by the number of neighboring Se around each Se atom. The open circles and crosses show the contributions to $f_{\mathrm{Se}}(Q)$ from Se atoms coordinated to two and one neighboring Se, respectively. The contribution from Se atoms that have no neighboring Se is shown by the solid circles. It is clearly seen that the asymmetric distribution of $f_{\mathrm{Se}}(Q)$ comes from the difference in the distribution of the three contributions. The profiles for the twofold- and onefold-coordinated Se atoms (open circles and crosses) shift toward smaller Q (larger $|Q|$) with increasing Tl concentration. At the equiatomic composition, the contribution from Se atoms without neighboring Se (solid circles) becomes finite, which corresponds to the appearance of negatively charged ions. The distribution range of this contribution is unchanged when the Tl concentration is increased.

In the liquid alkali-metal selenides,[17] the gross-charge distribution for alkali-metal atoms has a peak near the ideal value, $Q=1.0$, reflecting the fact that almost all s electrons of alkali-metal atoms are transferred to Se atoms. The asymmetric distribution of the gross charges of Se atoms comes from the coordination dependence of the gross charges similar to the Tl-Se system. However, there exist no contributions from negatively charged ions in the liquid alkali-metal selenide at the equiatomic composition.

IV. SUMMARY

We have investigated the concentration dependence of the structural and bonding properties of the liquid Tl-Se alloys by means of *ab initio* molecular dynamics simulations. It has been shown that the calculated structure factors are in good agreement with experiments over the whole range of Tl concentration. We have confirmed from the calculated electronic densities of states that the liquid Tl-Se alloys have semiconducting properties for Tl concentrations not exceeding the stoichiometric composition, while they are metallic for larger Tl concentrations. Based on the population analysis, we have clarified the changes in the bonding properties and the atomic charges due to the addition of Tl atoms. The differences of structural and electronic properties between the liquid Tl-Se and alkali-metal-chalcogen systems have also been discussed.

ACKNOWLEDGMENTS

The authors acknowledge fruitful discussions with Makoto Yao. The present work was supported in part by the Grant-in-Aid for Scientific Research on Priority Area, "Nanoionics (439)" from the MEXT, Japan. The authors thank the Supercomputer Center, Institute for Solid State Physics, University of Tokyo for the use of the facilities.

[1] *The Physics of Selenium and Tellurium*, Proceedings of the International Conference on the Physics of Selenium and Tellurium, Königstein, FRG, 1979, edited by E. Gerlach and P. Grosse (Springer, Berlin, 1979).
[2] Y. Nakamura and M. Shimoji, Trans. Faraday Soc. **65**, 1509 (1969).
[3] T. Usuki, J. Phys. Soc. Jpn. **62**, 634 (1993).
[4] V. Sklyarchuk and Y. Plevachuk, J. Alloys Compd. **327**, 47 (2001).
[5] T. Usuki, Y. Shirakawa, and S. Tamaki, J. Phys. Soc. Jpn. **61**, 2805 (1992).
[6] S. B. Lague, A. C. Barnes, A. D. Archer, and W. S. Howells, J. Non-Cryst. Solids **205-207**, 89 (1996).
[7] A. C. Barnes and C. Guo, J. Phys.: Condens. Matter **6**, A229 (1994).
[8] A. C. Barnes, S. B. Lague, M. A. Hamilton, H. E. Fischer, A. N. Fitch, and E. Dooryhee, J. Phys.: Condens. Matter **10**, L645 (1998).
[9] F. Kakinuma, S. Ohno, and K. Suzuki, J. Non-Cryst. Solids **250-252**, 453 (1999).
[10] Y. Tsuchiya, J. Phys. Soc. Jpn. **62**, 2698 (1993).
[11] Y. Ohmasa, S. Takahashi, K. Fujii, Y. Nishikawa, and M. Yao, J. Phys.: Condens. Matter **18**, 8449 (2006).
[12] Y. Ohmasa, S. Takahashi, K. Fujii, Y. Nishikawa, and M. Yao, J. Phys. Soc. Jpn. **75**, 084605 (2006).
[13] Y. Ohmasa, Y. Nishikawa, and M. Yao, J. Non-Cryst. Solids **353**, 3576 (2007).
[14] Ş. Ellialtıoğlu, E. Mete, R. Shaltaf, K. Allakhverdiev, F. Gashimzade, M. Nizametdinova, and G. Orudzhev, Phys. Rev. B **70**, 195118 (2004).
[15] G. Ferlat, A. San Miguel, H. Xu, A. Aouizerat, X. Blase, J. Zuñiga, and V. Muñoz-Sanjosé, Phys. Rev. B **69**, 155202 (2004).
[16] K. Kohary, V. M. Burlakov, D. G. Pettifor, and D. Nguyen-Manh, Phys. Rev. B **71**, 184203 (2005).
[17] F. Shimojo and K. Hoshino, Phys. Rev. B **74**, 104202 (2006).
[18] F. Shimojo, K. Hoshino, and Y. Zempo, Phys. Rev. B **59**, 3514 (1999).

[19] F. Shimojo, K. Hoshino, and Y. Zempo, Phys. Rev. B **63**, 094206 (2001).
[20] P. E. Blöchl, Phys. Rev. B **50**, 17953 (1994).
[21] G. Kresse and D. Joubert, Phys. Rev. B **59**, 1758 (1999).
[22] J. P. Perdew, K. Burke, and M. Ernzerhof, Phys. Rev. Lett. **77**, 3865 (1996).
[23] G. Kresse and J. Hafner, Phys. Rev. B **49**, 14251 (1994).
[24] F. Shimojo, R. K. Kalia, A. Nakano, and P. Vashishta, Comput. Phys. Commun. **140**, 303 (2001).
[25] F. Römermann, Y. Feutelais, S. G. Fries, and R. Blachnik, Intermetallics **8**, 53 (2000).
[26] S. Nosé, Mol. Phys. **52**, 255 (1984).
[27] W. G. Hoover, Phys. Rev. A **31**, 1695 (1985).
[28] M. Tuckerman, B. J. Berne, and G. J. Martyna, J. Chem. Phys. **97**, 1990 (1992).
[29] F. Shimojo, K. Hoshino, and Y. Zempo, J. Phys. Soc. Jpn. **72**, 2822 (2003).
[30] R. S. Mulliken, J. Chem. Phys. **23**, 1833 (1955).
[31] R. S. Mulliken, J. Chem. Phys. **23**, 1841 (1955).
[32] D. Sánchez-Portal, E. Artacho, and J. M. Soler, J. Phys.: Condens. Matter **8**, 3859 (1996).
[33] M. D. Segall, R. Shah, C. J. Pickard, and M. C. Payne, Phys. Rev. B **54**, 16317 (1996).
[34] The integration of $p_{\alpha\beta}(\bar{O})$, $\int_{O_{\min}}^{\infty} p_{\alpha\beta}(\bar{O})d\bar{O}$, gives the average number of β-type atoms that have overlap populations greater than $O_{\min}$ around one α-type atom.
[35] $f_\alpha(Q)$ is normalized as $\int f_\alpha(Q)dQ=1$.